ACS OMEGA

http://pubs.acs.org/journal/acsodf

Article

# Real-Time Monitoring of Selenium in Living Cells by Fluorescence Resonance Energy Transfer-Based Genetically Encoded Ratiometric Nanosensors

Reshma Bano, Mohd Mohsin,* Mohammad Zeyaullah, and Mohammad Suhail Khan

Cite This: *ACS Omega* 2023, 8, 8625−8633

Read Online

ACCESS | Metrics & More | Article Recommendations | Supporting Information

**ABSTRACT:** Selenium is a component of selenoproteins, which plays a crucial role in cellular redox homeostasis, thyroid metabolism, and DNA synthesis. Selenium has pleiotropic effects like antioxidant and anti-inflammatory activities; however, excess intake of selenium can imbalance such processes. The effects of selenium on human health are numerous and complex, demanding additional research to monitor the flux rate of selenium. Here, we have created a noninvasive and highly efficient genetically encoded fluorescence resonance energy transfer (FRET)-based nanosensor, SelFS (**Sel**enium **F**RET-**S**ensor), for real-time monitoring of selenium at the cellular and subcellular levels. The construct of the nanosensor contains a selenium-binding protein (SeBP) as the selenium-detecting element inserted between the green fluorescent protein variants enhanced cyan fluorescent protein and Venus. In the presence of selenium, SelFS brings a conformational change, which is seen in the form of FRET. *In vitro* studies showed that SelFS is highly specific and selective for selenium and stable at an altered pH range from 5.0 to 8.0. SelFS is a flexible and dynamic tool for the detection of selenium in both prokaryotes and eukaryotes in a noninvasive way, with a binding constant ($K_d$) of 0.198 × $10^{-6}$ M as compared to its mutants. The developed nanosensor can provide us a reporter tool for a wide range of industrial and environmental applications, which will help us to understand its functions in biological systems.

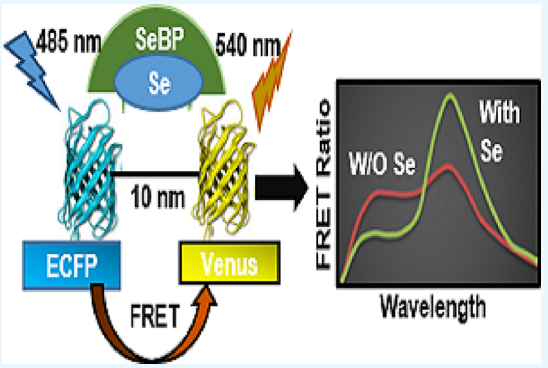


## 1. INTRODUCTION

Selenium (Se) is the most interesting element due to its clinical and environmental impacts. The necessity and toxicity of this element depend on the concentration and chemical forms in its availability in a given sample.[1] Selenium deficiency inhibits the expression of a number of enzymes that cause aberrant cell growth and diseases.[2] Selenium is unique as it is a vital dietary element for health and also toxic at comparatively low levels in the diet. The standard daily allowance for selenium is 55 $\mu$g/day for human. In the form of selenite, it works as a crucial micronutrient in the range of 0.1−0.2 $\mu$g/g in the diets of experimental animals, but it converts as toxic beyond 5 $\mu$g/g. The environmental concentration of selenium in the earth's crust is present in the range of 0.03 to 0.08 $\mu$g/g.[36,37] Selenium intake varies considerably around the globe, from low (related to selenium-deficiency conditions) to high levels (associated with garlic breath, hair loss, damaged nails, neurological disorders, poor dental health, and paralysis).[3] High levels of free selenium are harmful to cells as they negatively impact a number of their metabolic pathways. Long-term exposure of selenium effects has been reported to cause hypochromic anemia and leukopenia.[4] So, having enormous properties, there is a necessity to develop some reliable methods for studying the speciation of selenium in the environmental and biological samples to understand the biochemical cycle, mobility, and uptake of selenium and its toxicity.[5] There are several analytical procedures for detecting selenium in various kinds of samples such as gas chromatography, X-ray fluorescence, and polarography useful to detect selenium compounds under specific circumstances.[6] Besides these, some other techniques like a spectrophotometric method, atomic fluorescence and absorption spectrometry, chemiluminescence, and a gold nanoparticle-based colorimetric method have also been used.[7,8] Still, most of these approaches include expensive devices or time-consuming procedures. Thus, it is highly desirable to design a rapid and easy method for real-time detection of selenium. A group of researchers developed an Ag nanoprism-based plasmonic sensor for the detection of selenium. They established a simple and sensitive colorimetric sensor to analyze the trace amount of selenium in actual samples with satisfactory

Received: December 7, 2022
Accepted: February 10, 2023
Published: February 22, 2023

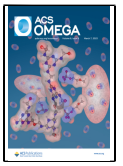





https://doi.org/10.1021/acsomega.2c07809
*ACS Omega* 2023, 8, 8625−8633

outcomes.[9] Another researcher also developed a TP-fluorescence resonance energy transfer (FRET)-based ratiometric probe, CmNp-Sec, for visualization of selenocysteine (Sec) derivatives. In this study, the CmNp-OH was created with a non-conjugated linker using a two-photon fluorophore coumarin derivative (as a donor) and a naphthalimide fluorophore (as an acceptor). The probe CmNp-Sec was efficiently illustrative in tracing Sec in living tissues and zebrafish.[10] Although the above sensors for evaluating selenium are dye based, these can be used *in vitro* generally with low brightness that precludes tracking of a flux of ions with high time resolution. However, fluorescent proteins are best at tracking metals in live cells, exclusively with super-resolution microscopy. On the other hand, several methods occur to progress the brightness of the target metal by genetically pairing numerous fluorescent proteins together.[11,12] It is recognized that fluorescent proteins have great potential applications to appear as ultimate tools in the arena of bioimaging study and monitoring analytes like metals, nutrients, amino acids, and others in biosystems. Many genetically encoded sensors have been developed using these proteins, for example, SenALiB for arsenic, SenSil for silver, FLIP-Leu for lysine, etc.[24,25,34] Meanwhile, they can endorse noninvasiveness, rapid response, high selectivity, specificity, and sensitivity, as well as high spatiotemporal resolution.[13] Thus, we have reported a genetically encoded FRET-based nanosensor for detecting and monitoring the flux of selenium in the living cells. Two red-shift variants of green fluorescent protein (GFP), enhanced cyan fluorescent protein (ECFP) as a donor and Venus (a mutated yellow fluorescent protein) as an acceptor, were attached at the N-terminus and C-terminus, respectively, with the selenium-binding protein to create the nanosensor. The developed nanosensor exhibits the concentration-dependent flux of selenium within the cells, allowing us to understand the physical distribution of selenium at the cellular and subcellular levels within the organisms at high spatiotemporal resolution. This sensor can be helpful in real-time detection of selenium in metabolic pathways within the prokaryotic and eukaryotic organisms at the cellular and subcellular levels.

## 2. RESULTS

**2.1. Development, Expression, and Isolation of the Sensor Protein.** A binding partner of selenium, that is, SeBP, has been chosen to create a genetically encoded FRET-based sensor to monitor the selenium level within the living cells. For generating a FRET-based nanosensor, the fluorescent variants ECFP (donor) and Venus (acceptor) were attached with the SeBP at the N- and C-termini, respectively, to attain a recombinant protein.[14−16] The linear arrangement of the restriction sites and the construction of the selenium nanosensor are shown in Figure 1A. SeBP protein is a suitable biomolecule for FRET-based investigations due to its sandwiched selenium-binding cleft and conformational elasticity within its structure. When selenium binds to the ligand-sensing domain (SeBP), conformational changes are triggered that alter the distance between the two fluorophores, resulting in a signal known as FRET, as shown in Figure 1B. Sensor's protein was expressed in *Escherichia coli* BL21-Codon Plus after transformation with the construct's plasmid, and cells were induced with 0.5 mM isopropyl-D-1-thiogalactopyranoside (IPTG). Expressed recombinant protein was successfully purified using nickel-nitrilotriacetic acid (Ni-NTA) His-tag

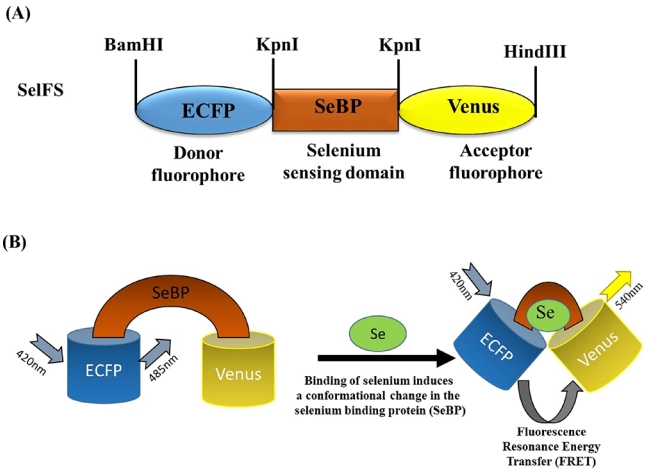


**Figure 1.** Genetically encoded nanosensor's design and schematic representation. (A) A linear demonstration of the nanosensor construction is shown schematically. (B) In the presence of selenium, ECFP and Venus approach one another, exhibiting a FRET signal.

affinity columns. Through the histidine imidazole ring, His-tags bind to the immobilized metal, and attached tagged protein can be easily removed using elution solution containing imidazole (100−250 mM).[17] Using 10% sodium dodecyl sulfate-polyacrylamide gel electrophoresis (SDS-PAGE), the fidelity of the chimeric protein was examined and verified.

**2.2. SelFS Protein Fluorescent Emission Spectra.** Different concentrations (5 and 10 $\mu$M) of selenium were used to measure the shift in the emission spectrum (Figure 2).

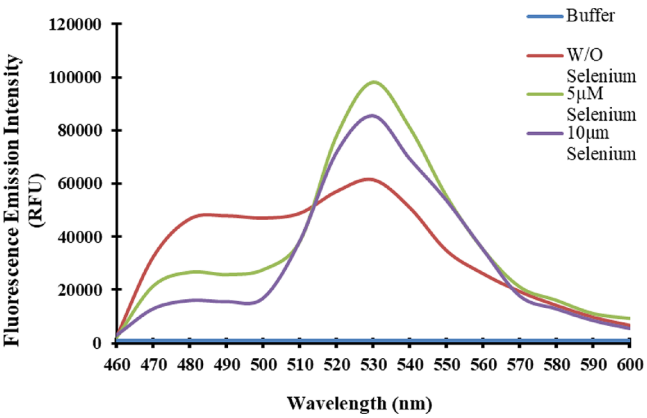


**Figure 2.** Spectral evaluation of the FRET-based sensor *in vitro*. The nanosensor's emission spectrum was captured between 460 and 600 nm in wavelength. With the addition of selenium, the relative fluorescence emission intensities of the donor and acceptor fluorophores are altered.

With the addition of selenium with the SelFS protein, ECFP and Venus's emission spectral profiles indicate relevant variation in the emission intensities. After adding selenium, the SeBP undergoes a conformational change that brings the two fluorophores (ECFP, the donor, and Venus, the acceptor) together to transfer the maximum energy from donor to acceptor fluorophore. As a result, the emission intensity of Venus increases, whereas the emission intensity of ECFP decreases.[18]

**2.3. Examining the Stability of the Nanosensor.** The stability of the nanosensor was examined by the presence of


https://doi.org/10.1021/acsomega.2c07809
ACS Omega 2023, 8, 8625−8633

various buffers such as Tris buffer saline (TBS), 3-(*N*-morpholino)propanesulfonic acid (MOPS), and phosphate-buffered saline (PBS). The SelFS protein was taken into account by the FRET method in different buffers with altered pH values ranging from 5.0 to 8.0 as variations in the emission intensity ratio (540/485 nm). Among all the buffers, SelFS shows nonsignificant deviations in the dual emission intensity ratio only in PBS buffer (Figure 3A). For further experimental tests, the sensor protein was diluted in 20 mM PBS buffer with physiological pH. The fluorescence emission intensity ratio was measured using a monochromatic microplate reader with and without selenium. The nanosensor protein exhibits significant changes in the FRET ratio up to pH 6.5 in the presence of selenium (5 $\mu$M), indicating the sensor protein's sensitivity in the acidic range. The sensor's stability in the alkaline environment was confirmed by the nonsignificant changes in the fluorescence emission intensity ratio that was occurred in an alkaline pH range (Figure 3B).

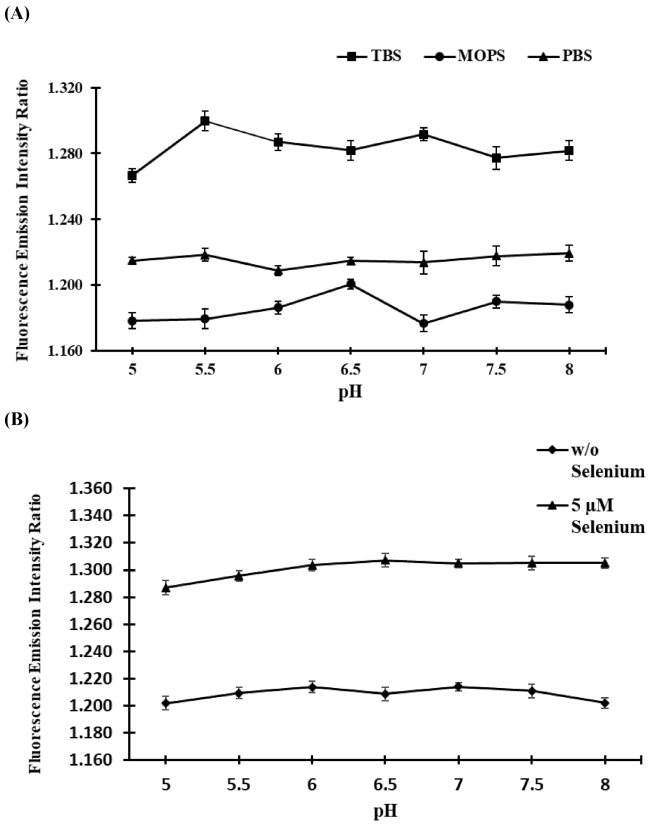


**Figure 3.** Buffer stability analysis. (A) Different pH ranges of MOPS, PBS, and TBS were used to measure the emission intensity ratio at 540/485 nm wavelength. With 20 mM PBS buffer, the SelFS sensor was discovered to be in a stable state because PBS buffer showed the least amount of change in the FRET ratio. (B) Both without and with the addition of 5 $\mu$M selenium, the stability of the SelFS sensor was examined in PBS buffer in the physiological pH range (5.0 to 8.0). The means of three independent replicates are used to express the data points ($n$ = 3).

**2.4. Analysis of Specificity and Selectivity of the Sensor Protein.** To test the specificity of the nanosensor, titration of the SelFS was determined using a 96-well plate reader. We experimented with various metals like silver, iron, tungsten, and arsenic using different concentrations such as 10 nM, 100 nM, 200 nM, 500 nM, 1 $\mu$M, 5 $\mu$M, and 10 $\mu$M each. A significant change in the fluorescence emission intensity ratio was detected using a microplate reader with the presence of selenium (5 $\mu$M) compared to control (absence of selenium) (Figure 4A). The SelFS was not exhibiting any appreciable variations in the FRET ratio with the presence of other metals. To test the effect of essential metal ions ($Na^+$, $K^+$, $Ca^{2+}$, and $Mg^{2+}$) on the specificity and selectivity of the SelFS protein, 160 $\mu$L of the purified sensor protein was mixed with 20 $\mu$L of the biological concentration of these metal ions and 20 $\mu$L of 5 $\mu$M selenium in each of the 96-well plates. As a result, a nonsignificant change has been observed in the FRET ratio that shows that selenium sensing is not effected when these metals coexist in biological systems (Figure 4B).

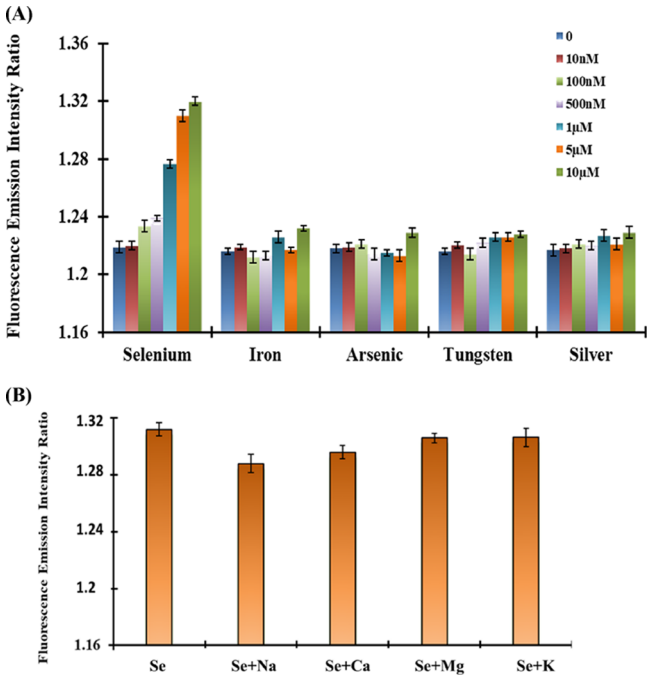


**Figure 4.** Characterization of the SelFS *in vitro* assay. (A) The purified SelFS protein's metal ion selectivity was assessed in the presence of several metals (iron, arsenic, tungsten, and silver), producing the greatest change in the fluorescence emission intensity ratio with selenium. (B) Variation of the acceptor-to-donor fluorescence ratio following the addition of possible intracellular irritants such as NaCl, KCl, $CaCl_2$, and $MgCl_2$. Three independent replicates ($n$ = 3) are used to get the means for the data points. The standard deviation is shown by vertical bars.

**2.5. Affinity Mutants of SelFS.** A total of three mutants, I29R, K42W, and D61C, were engineered through offering point mutations covering an array of selenium with different concentrations from nanomolar to micromolar. Mutations were confirmed by sequence analysis (Figure S1). Evaluated to the SelFS-WT sensor, with a $K_d$ of 0.1984 $\mu$M, the mutants I29R, K42W, and D61C with $K_d$ of 1.598, 3.884, and 3.608 $\mu$M, respectively, have a low affinity toward selenium (Table 1).

Hence, among all the created mutant sensors, the SelFS-WT sensor was measured outstanding for studying the dynamics of selenium levels. A sigmoid saturation curve was acquired that initially signifies the maximum change in the FRET ratio till 20 $\mu$M selenium concentration and saturated afterward at 50 to 200 $\mu$M selenium (Figure 5).



https://doi.org/10.1021/acsomega.2c07809
ACS Omega 2023, 8, 8625−8633

**Table 1. Binding Constant ($K_d$) and Dynamic Range of SelFS-WT and the Sensor's Mutant[a]**

| name of the nanosensor | mutation | $K_d$ ($\mu$M) (±SD) | dynamic range ($\mu$M) |
|---|---|---|---|
| SelFS | WT | 0.1984 (±0.003) | 0.05−60 |
| SelFS-29 | I29R | 1.598 (±0.002) | 0.11−95 |
| SelFS-42 | K42W | 3.884 (±0.001) | 0.03−140 |
| SelFS-61 | D61C | 3.608 (±0.002) | 0.075−150 |

[a]SD = standard deviation.

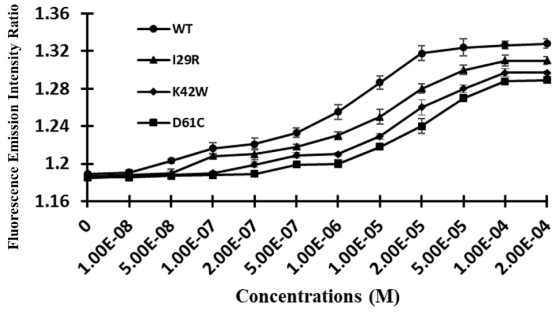


**Figure 5.** *In vitro* FRET emission of WT and mutant sensors altered in the presence of selenium. I29R, K42W, and D61C affinity mutants were produced and compared with the SelFS (WT) sensor protein. The data represent the averages from three separate replications ($n$ = 3). The standard error is displayed by vertical bars.

**2.6. *In Vivo* Monitoring of Selenium in Prokaryotic Cells.** Using a confocal microscope, live-cell imaging was captured with a successful expression of SelFS in the *E. coli* cells (Figure S2). With the addition of 5 $\mu$M selenium, the *in vivo* bacterial assay was carried out for 90 min in a microplate reader and asserted the change in the FRET ratio with an interval of 5 min. Thus, on the addition of 5 $\mu$M selenium, a substantial escalation in the FRET ratio was recorded up to 52 min, which subsequently saturated (Figure 6). The FRET ratio

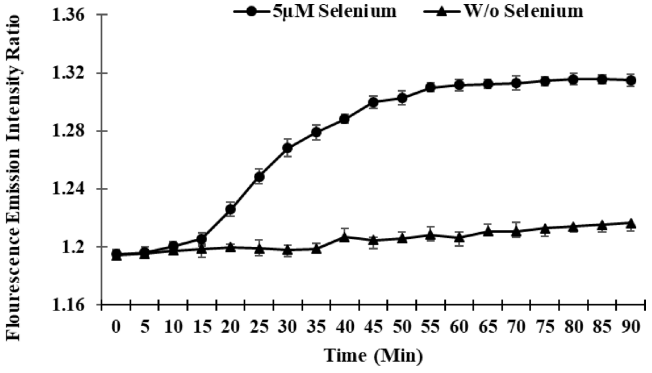


**Figure 6.** Selenium uptake monitoring in bacterial cells. The time-dependent response curve was obtained by measuring the FRET ratio after the incubation of bacterial cell suspension containing SelFS with 5 $\mu$M selenium. The data are the means of three independent replicates ($n$ = 3). The vertical bars indicate the standard error.

did not change significantly in the absence of selenium. The experiment was carried out in triplicates for the monitoring of the selenium flux in bacterial cells in real time, and the results demonstrate the feasibility of SelFS.

**2.7. Synchronized Monitoring of Selenium in Yeast.** As a eukaryotic model system, *Saccharomyces cerevisiae* was preferred to evaluate the flux rate of selenium. The construct of the nanosensor was transferred by gateway cloning in the yeast vector pYEST-DEST52 (Invitrogen). Here, the construct of the SelFS nanosensor performed its efficacy after being transformed in the yeast cells for expression. Ratiometric images of transformed *S. cerevisiae* with the construct of SelFS using a Leica confocal microscope presented an extremely fluorescent cytosol representative of the expression of the nanosensor and an unstained vacuole present in the cytosol without the expression of the nanosensor (Figure 7A).

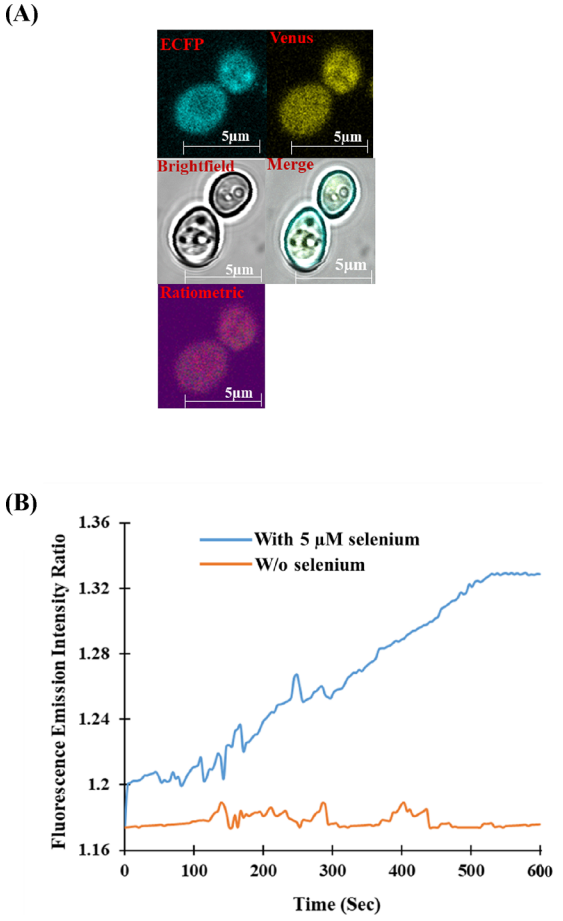


**Figure 7.** Measuring the uptake of selenium by yeast cells in real time. (A) Confocal image demonstrating the SelFS expression in the *S. cerevisiae* yeast cell cytoplasm (scale bar: 5 $\mu$m); the cyan color and yellow color are showing the expression of ECFP and Venus fluorophores, respectively. (B) In the presence of 5 $\mu$M selenium, the graph depicts a change in the 540/485 nm ratio within the cytoplasm compared with control (without selenium) of a single yeast cell expressing SelFS.

Selenium (5 $\mu$M) was added with the expressing yeast cells under the confocal microscope, and changes were recorded in the fluorescence emission intensity ratio (Figure 7B). The fluorescence emission intensity ratio significantly increased from 1.175 at 0 s to 1.328 at 600 s and gets saturated, while nonsignificant changes were obtained in the ratio without selenium as the control. After background subtraction, it was preferred to determine the emission intensity ratio for the ROI by using the emission tool of the LAS-AF software to present the data.

**2.8. Monitoring of Selenium Uptake by SelFS in HEK-293T Cells.** To assess the level of selenium absorption and dispersion *in vivo*, SelFS was transfected in human embryonic


https://doi.org/10.1021/acsomega.2c07809
ACS Omega 2023, 8, 8625−8633

kidney (HEK-293T) cells. SelFS was primarily distributed in the cytoplasm of transfected cells, as seen in confocal images of the sensor-expressed HEK-293T cells (Figure 8A). With the

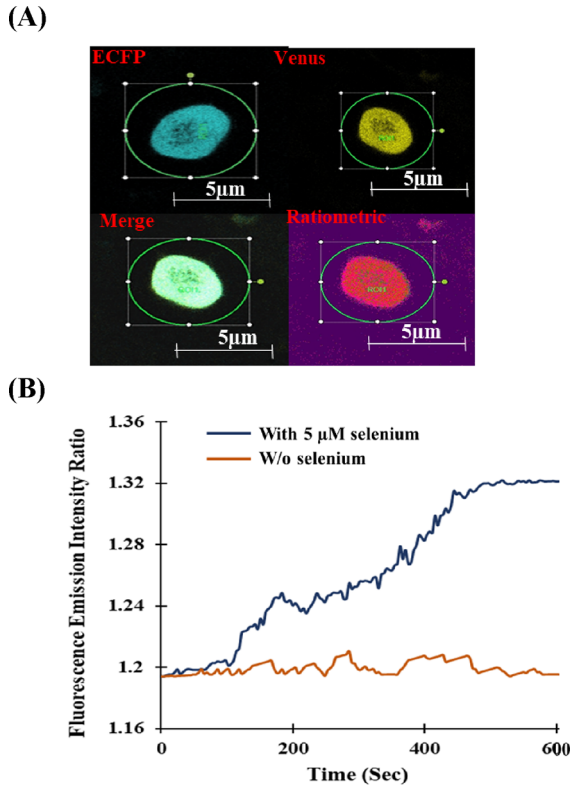


**Figure 8.** SelFS in the HEK-293T cell line in real-time imaging. (A) Confocal images of the HEK-293T cell line demonstrate SelFS expression in the presence of selenium (scale bar: 5 $\mu$m); the cyan color and yellow color are showing the expression of ECFP and Venus fluorophores, respectively. (B) SelFS was transfected into HEK-293T cells, and the changes in the emission intensity ratio were monitored for the specific time period. The graph shows the 10 min shift in the Venus/ECFP ratio.

presence of selenium, the Venus emission intensity significantly increases, which results in a time-dependent decrease in the ECFP emission intensity in the cells. As a result, there is a time-dependent increment in the Venus/ECFP emission intensity ratio compared with control; nonsignificant changes in the emission intensity ratio were obtained (Figure 8B). The fluorescence emission intensity ratio (540/485 nm) was recorded and found to be 1.19 at the base level and to rapidly increase after the addition of 5 $\mu$M selenium and reaching 1.320 at a saturation level after 480 s.

**2.9. Cytotoxic Investigation.** To conclude the cytotoxicity of a high dose of selenium *in vivo*, the 3-[4,5-dimethylthiazol-2-yl]-2,5-diphenyltetrazolium bromide (MTT) assay was carried out. Cell toxicity experiments were accomplished for 24 h exposure of different concentration ranges (0−50 $\mu$M) of selenium. In cytotoxic analysis, no effect on morphology and no toxic impact were found on HEK-293T cells during the short period of selenium exposure (Figure 9). But it becomes harmful when the exposure time extends. So, only a high concentration of selenium (>10 $\mu$M) toxicity to HEK-293T cells occurred during the cell viability test.

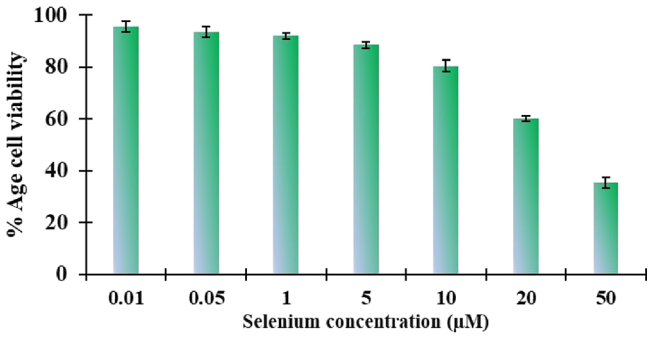


**Figure 9.** A study on HEK-293T cells using selenium to determine cell viability. The 3-[4,5-dimethylthiazol-2-yl]-2,5-diphenyltetrazolium bromide (MTT) assay was used to test the vitality of HEK-293T cells, and the selenium content was increased.

## 3. DISCUSSION

Selenium is a vital trace element and micronutrient for humans and other animals. Numerous health conditions, including immunological inadequacy, are associated with selenium deficiency. It is well known that certain selenoproteins need selenium assistance to be expressed, such as the inclusion of selenocysteine *via* tRNA.[2] Also, it has important antiaging, anticancer, and detoxifying roles,[19] and it safeguards the immune system's cellular components. Therefore, to better determine the level of selenium in living cells and understand how it is distributed, we need a device with a practical and simple approach for monitoring selenium levels *in vivo*. Figure 1A is an illustration of the construction of a selenium nanosensor, together with the linear organization of restriction sites. SeBP protein is a suitable biomolecule for FRET-based investigations due to its sandwiched selenium-binding cleft and conformational elasticity within its structure. The two domains of the SeBP protein undergo these conformational changes as a result of selenium binding, which contribute to improved FRET efficiency. Venus is distant from ECFP in the open state compared to the closed state, which results in a reduced energy transfer from the donor to acceptor. When selenium binds to the ligand-sensing domain, SeBP, conformational changes are triggered that alter the distance between the two fluorophores, resulting in a signal known as FRET, as shown in Figure 1B. The *Aequorea victoria*-GFP (Av-GFP) spectral variants ECFP and Venus were employed to get ratiometric changes with the flux of selenium in the live cell. Several experiments have been conducted in recent years using various organic dyes, probes, and quantum dots to build sensors for monitoring of selenium. However, because they contain organic fluorescent probes, which are extremely toxic and difficult to introduce into cells, these fluorescent-conjugated nanosensors stress out living cells.[20,21] Thus, to limit the detrimental effects of these chemical and hazardous dyes, we have applied an alternative required strategy using spectral variations of GFP.

SeBP, a subunit of an 8.8 kDa oligomer with an asymmetric pentamer shape, is the binding partner of selenium. NMR spectroscopy was used to determine the solution structure of SeBP. Each of SeBP's five subunits is composed of a four-stranded twisted sheet on top of the $\alpha$-helix. Hydrogen bonding and hydrophobic interactions play a major role in the constancy of all subunits. The amino acid Cys59 has been shown to be important for selenium binding, elastic, and accepting of a variety of conformations. However, the accessibility of cysteine is confined in the structure, eliminating


https://doi.org/10.1021/acsomega.2c07809
ACS Omega 2023, 8, 8625−8633

the binding of free selenium readily.[22] Selenium reactivity, however, relies on a single cysteine (Cys59) in the $\beta3-\beta4$ loop of SeBP. The interaction of the selenium with the mainly hydrophobic residues bordering the core is required for access to the Cys59 from either side of the SeBP core. Due to the close proximity of the two lobes of the SeBP in a *Venus flytrap* arrangement, the binding of selenium to the SeBP causes conformational alterations. This ultimately satisfies the conditions of FRET for occurrence by bringing the fluorophore pairs within close proximity of about 10 nm. This is because the FRET is dependent on the distance, the orientation of the fluorophores (dipole−dipole orientation), and the overlap of the spectral lines from the donor's emission and acceptor's absorption.[23−25] The N- and C-termini of SeBP, which are located at the distal extremities of the two lobes, should come together upon selenium binding, enhancing the fluorescence emission intensity ratio. Therefore, as ligands are added, the construct should move, which could alter the relative orientation of the connected fluorophores' transition dipoles and change the FRET ratio.[15,26] A change in the fluorescent protein's emission spectrum after selenium addition was detected by spectral analysis, indicating that the selenium-binding domain's conformation changed to bring the two fluorophores together and cause FRET. In the absence of selenium, no modification in the analysis of the emission spectra was observed. The ecological pH is another important consideration when using FRET imaging to assess the stability of the construct. Particularly, pH has an impact on the ratiometric signals of CFP−YFP pairings, which may enable the fidelity of the corresponding signal when used in situations with fluctuating pH. When the pH is changed from 7.5 to 5, the AKAR biosensor for protein kinase A (PKA) activity experiences a 40% FRET ratio drop. In contrast, kinase activity typically causes a 10−20% ratio change in the average FRET change. EYFP and its variant Venus appear to be extremely pH-sensitive FRET acceptors, and coupling any of these YFP acceptors with a pH-insensitive donor would not significantly reduce agitations to lifetime or ratiometric signals.[27,28] Venus, an EYFP variant, is brighter, is less sensitive to the environment, and has a substantially lower $pK_a$ (6.0), making it a suitable acceptor for environments with acidic or alkaline conditions.[29] To extend the physiological exposure range of the SelFS nanosensor to selenium, affinity mutants of the nanosensor were created. Point mutation sites were chosen at random. These three mutants were made by substituting chosen residues with hydrophobic, polar, and aromatic residues. The main objective was to alter these residues to improve the conformational stability of the protein. To track and analyze changes in the FRET ratio with the selenium in real time, SelFS was expressed in the cytoplasm of bacterial cells. As a result, a considerable increase in the FRET ratio was observed upon the addition of 5 $\mu$M selenium up to 52 min before it becomes saturated. The FRET ratio change was not significant in the absence of selenium. Numerous genetically encoded nanosensors have been developed with great specificity and selectivity for measuring the level and flux of various analytes.[15] Ratiometric imaging of the *S. cerevisiae* cells revealed that selenium is carried into the cytoplasm and is then taken up by the SelFS sensor, which produces a signal in the form of the FRET ratio. The recorded study indicates that the emission intensity ratio abruptly increased up to 450 s and further increased until it reached saturation after the addition of selenium. The SelFS is successfully occupied in the eukaryotic cells, according to confocal imaging of the cells that are expressing it. As demonstrated by Met-cad, SenVital, and cAMP,[30−32] certain other genetically encoded nanosensors recently reported have a remarkable capacity to detect and localize metabolites like metals in subcellular components of a HEK-293T cell. When describing the mechanism involved in selenium uptake, transient transfection in HEK-293T cells with SelFS expresses the highest ability of this genetically encoded nanosensor. According to the results obtained from the SelFS transfected cells, the SelFS has a remarkable potential to research the real-time dynamics of selenium in human cells *in vivo*. Selenium is a necessary element for normal cellular functions, but too much of it in dietary supplements can be hazardous. With either acute or long-term ingestion of a large dosage of selenium, toxicity can develop. The most obvious signs of exposure to high selenium levels include acute weakness, brittleness, joint pain, nausea, weariness, and the odor of garlic in one's breath.[1,33]

## 4. CONCLUSIONS

An asset of FRET biosensing over conventional biochemical methods is that it is accomplished optically and enables the imaging of live cells in a nondestructive and noninvasive way. We have established an economical, simple, highly sensitive, and selective fluorescence-based biosensor to monitor and quantify selenium levels. The developed biosensor can detect and assess the cellular levels of selenium. The expression of SelFS was determined by confocal imaging of bacterial cells and eukaryotic cells. This sensor has been demonstrated that the genetically encoded nanosensor SelFS is a powerful tool for monitoring the level and flux rate of selenium in bacteria, yeast, and HEK-293T cells. The developed nanosensor would be helpful to understand the uptake and assimilation of selenium in the metabolic pathways of living organisms.

## 5. METHODS AND METHODOLOGY

### 5.1. Designing and Construction of the Nanosensor.

The crystal structure of selenium-binding protein (SeBP; PDB ID-2JZ7) was retrieved from the RCSB Protein Data Bank (PDB) along with the gene and amino acid sequence from the Kyoto Encyclopedia of Genes and Genomes (KEGG) database. The selenium-binding protein, SeBP, in *Methanococcus vannielii* mediates selenium transport inside the cell. During transport, SeBP sequesters selenium, regulating the amount of free selenium in the cell, and delivers it specifically to the selenophosphate synthase enzyme.[22] SeBP was a signal peptide-free protein confirmed by using the Signal P4.1 server (CBS, Denmark). Using a set of primers, the SeBP gene was amplified by polymerase chain reaction (PCR) from the genomic DNA of *M. vannielii*. The reverse primer sequence 5′-CGGggtaccCCTACTCCGCGTCAAATGGTACCGC-3 and the forward primer sequence 5′-CGGggtaccTTCGAGGA-CAAATTCATTATCACCA-3 both introduce a restriction site *Kpn*I on either side of the start codon and after removing the stop codon, respectively. DNA sequences of ECFP and Venus were amplified by PCR after shortening the 5′ and 3′ ends to four codons and two codons each, respectively. The ECFP and Venus fluorophores were attached to a bacterial expression vector called pRSET-B (Invitrogen, USA) to create a cassette (Figure S3). For a nanosensor construct pRSET-B_ECFP_SeBP_Venus, inserting the amplified SeBP gene between ECFP and Venus in the pRSET-B vector and fidelity


https://doi.org/10.1021/acsomega.2c07809
ACS Omega 2023, 8, 8625−8633

of the construct was confirmed by full-length sequencing (Figure S4). The pYES-DEST52 vector was used to carry the ECFP_SeBP_Venus sequences by a gateway cloning method utilizing the LR-Clonase-II enzyme (Invitrogen, USA) following the manufacturer's instructions[34] for expression of the sensor protein in yeast. The *S. cerevisiae*/URA3 strain BY4742 was used for transforming the pYDEST-ECF-P_SeBP_Venus plasmid as a eukaryotic expression system. BY4742 strains were grown in liquid YEPD (yeast extract peptone dextrose) agar medium at 30 °C with aeration in a shaker. Following the manufacturer's instructions (Invitrogen, USA), competent cells of *S. cerevisiae*/*URA3* were prepared and used for transforming with the nanosensor sequences. The pcDNA3.1 (−) vector (Invitrogen) was used to express the sensor protein in HEK-293T cells for mammalian expression. By using the expression vector pRSET-B, the chimeric sequence was cloned in the pcDNA3.1 (−) vector at the *Hind*III and *Bam*HI sites.

**5.2. Expression and Purification of the Nanosensor.** The plasmid ECFP_SeBP_Venus construct was transformed utilizing the heat shock method developed by the calcium chloride chemical method in the bacterial cell *E. coli* BL21-Codon Plus strain. For bacterial expression, the cells containing 100 μg/mL ampicillin were cultured in Luria-Bertani (LB) media at 20 °C and 160 rpm within an aeration shaker. When the cells reached an optical density ($OD_{600}$) of between 0.4 and 0.6, 1 mM isopropyl-D-1-thiogalactopyranoside (IPTG) (Himedia) was added to induce the expression of the nanosensor protein. After induction, the cells were given additional 20 h of growth in darkness at 20 °C. Then, the cells were harvested to complete separation of the expressed bacterial cells using a refrigerated centrifuge (Thermo Scientific, USA) at 4500 rpm for 45 min and resuspended the cell pellet in a buffer (20 mM Tris−Cl, pH 7.8). Cells were lysed by ultrasonication (Sonics, USA) for 5−6 min with intervals of 15 s pauses. Lysed bacterial cells were centrifuged at 4500 rpm for 20 min to get rid of any cell debris. The collected supernatant of cell-free lysate was transferred to a nickel-nitrilotriacetic acid (Ni-NTA) resin (Qiagen, Germany) that was packed in a His-tag column (BioRad, CA, USA). For proper binding of the recombinant His-tagged sensor protein to the Ni-NTA resin, the column was incubated at 4 °C. After 1 h, the column was washed with a chilled 20 mM Tris−Cl and 10 mM imidazole buffer with pH 8.0. The purified recombinant sensor protein was eluted with an elution buffer of 20 mM Tris−Cl and 300 mM imidazole with pH 8.0. A higher concentration of imidazole was used in elution buffer to compete with the His-tag on the sensor protein for binding to the Ni-NTA resin. To ensure appropriate folding of the purified sensor protein, SelFS, a recombinant protein, was kept at 4 °C for an overnight duration.

**5.3. *In Vitro* Study of SelFS.** *5.3.1. Emission Spectral Analysis of SelFS.* A monochrome microtiter plate reader (Synergy H1, BioTek, USA) was used to analyze the fluorescence emission spectrum of the purified sensor protein using 485/20 and 540/20 nm emission intensities as the donor and acceptor, respectively, in the wavelength range of 460−600 nm with the presence and absence of selenium, which is taken from selenium dioxide ($SeO_2$; Himedia).

*5.3.2. Evaluating SelFS's pH Stability.* The kinetics of SelFS were first investigated in different buffer systems, including 20 mM PBS, Tris-buffered saline (TBS), and 3-(*N*-morpholino)-propanesulfonic acid (MOPS), in environments with varying pH levels from acidic to alkaline. To use a monochromatic microplate reader to track changes in the FRET ratio (540/485 nm) at various pH values, the SelFS was diluted numerous times in different buffers (PBS, MOPS, and TBS). The SelFS protein was tested using the PBS medium in the pH values of 5.0−8.0 both with and without addition of selenium in further experiment to determine the stability of the purified protein. A microplate reader monitored the ratiometric changes using an excitation filter of 420/20 nm and the wavelength of the FRET ratio ($Venus_{540/20nm}/ECFP_{485/20\ nm}$) after adding 5 μM selenium.

*5.3.3. Specificity and Impact of Various Biological Metals.* To determine the metal ion specificity of the SelFS protein, various metals were used in response to the change in the emission ratio (540/485 nm) on a microplate reader. The FRET ratio was recorded after adding selected metals using 180 μL of the SelFS protein (diluted in 20 mM PBS buffer pH 8.0) with 20 μL of selenium, silver, iron, tungsten, and arsenic metals in the nanomolar-to-micromolar range, 10 nM, 100 nM, 500 nM, 1 μM, 5 μM, and 10 μM. To perform the competitive experiments, the FRET (540/485 nm) ratio was recorded by adding the interferents such as $Ca^{2+}$, $Mg^{2+}$, $Na^{+}$, and $K^{+}$ to the SelFS protein in the presence of 5 μM selenium. The FRET ratio was detected after mixing 20 μL of these metals to 160 μL of the diluted SelFS protein with 20 μL selenium on a microplate reader.

*5.3.4. Affinity of SelFS and Generation of Affinity Mutants.* The binding constant ($K_d$) was calculated using GraphPad Prism software by fitting the ligand-titration curve in the binding isotherm equation: $S = (r-r_{apo})/(r_{sat}-r_{apo}) = [L]/(K_d + [L])$, where $S$ is the saturation, $[L]$ is the ligand concentration, $r$ is the ratio, $r_{apo}$ is a ratio in the absence of ligand, and $r_{sat}$ is the ratio at saturation.

Point mutations were added to the SelFS gene to produce mutants that would increase the sensor's physiological detection array. The structure of SeBP was acquired from the PDB to determine the amino acid residues present in the protein's binding pocket that facilitate selenium binding.[22] Using the QuikChange site-directed mutagenesis kit from Agilent USA, three mutants were produced by replacing the amino acid residues at positions 29 (isoleucine), 42 (lysine), and 61 (aspartate) with arginine, tryptophan, and cysteine, respectively. All these mutants of the SelFS protein were expressed and purified as described above for further analysis. SelFS was also utilized for *in vivo* selenium flux measurement investigations.

**5.4. *In Vivo* Monitoring of Selenium.** *5.4.1. Real-Time Monitoring of Selenium in Bacteria.* *E. coli* BL21-Codon Plus strain was transformed by nanosensor construct for expression. Cells were induced after growing at 37 °C with an $OD_{600}$ of between 0.4 and 0.6 to a final concentration of 1 mM IPTG and further grown in the dark for the next 16 h at 20 °C.[14] The bacterial cell suspension (180 μL) was prepared by resuspending the cell pellet in 20 mM PBS buffer and mixing with 5 μM selenium (20 μL) and then dispensing in each of the 96-well microplates with triplicates. The FRET signal was recorded for 90 min at regular intervals of 5 min using a monochromator microplate reader. After adding 5 μM selenium, the FRET ratio (540/485 nm) rises quickly up to an assured time before reaching saturation and becoming constant (Figure 6). The expressed bacterial cells were treated with 5 μM selenium and then fixed on a pre-coated poly-L-lysine glass slide. Using a confocal microscope (Leica,


https://doi.org/10.1021/acsomega.2c07809
ACS Omega 2023, 8, 8625−8633

Germany) outfitted with a TCS-SPE confocal head, 63 objective piece, cooled charge-coupled camera, and 1.53 NA LAS-AF software, FRET imaging of SelFS was carried out without background subtraction. A 420 nm excitation filter and two emission lasers (485 and 540 nm for ECFP and Venus, respectively) were used to measure dual emission intensities.

*5.4.2. Real-Time Screening of Selenium in Yeast Cells.* The SelFS was expressed in yeast cells using the *S. cerevisiae*/URA3 strain BY4742. Using the gateway technique, the construct ECFP_SeBP_Venus was transferred to the vector pYES-DEST52 that included the GAL1 promoter. These cells were grown for 3−5 days at 30 °C with aeration in a shaker incubator using a synthetic medium (SD) enriched with 2% sucrose and 3% galactose as such an inducer. Utilizing a confocal microscope (Leica DMRE) and LAS-AF software (Leica, Wetzlar, Germany), the sensor's expressed yeast cells were ratiometrically imaged. The FRET ratio change was recorded using two emission filters (485/20 and 540/20 nm for ECFP and Venus, respectively) and a 420/20 nm excitation filter. Following the addition of 5 $\mu$M selenium, the FRET ratio was observed for 10 min. The region of interest (ROI) was chosen to assess the real-time changes in the intensity ratio.

*5.4.3. Monitoring of Selenium Uptake by SelFS in HEK-293T Cells.* The ECFP_SeBP_Venus construct was transferred to the mammalian expression vector pcDNA3.1 (−) (Invitrogen, USA) for real-time monitoring of selenium in mammalian cells. For this study, human embryonic kidney (HEK-293T) cells were cultured and maintained in Dulbecco's modified Eagle's media (DMEM, Sigma, USA) with 50 $\mu$g/mL ampicillin and 10% heat-inactivated fetal bovine serum (FBS). Cultures were regularly maintained at 37 °C in a humidified incubator (5% $CO_2$). For further studies, sterile poly-L-lysine-coated coverslips were used in a 6-well culture plate for further growing cells. Transient transfection of cells with the pcDNA_ECFP_SeBP_Venus construct for the expression of the SelFS nanosensor in mammalian cells was carried out using Lipofectamine reagent. Through confocal microscopy (excitation 420/20 nm; emission laser filter 485/20 and 540/20 nm for ECFP/Venus, respectively), the images of expressed cells with SelFS were obtained. The emission intensity of Venus increased with time after adding the selenium, and the ECFP emission intensity decreased. So as with added 5 $\mu$M selenium, an increased FRET ratio was recorded in a time-dependent approach. Inside the cellular and subcellular compartments, expressed genetically encoded FRET-based nanosensors like SelFS have been demonstrated to permit localization and detection of a metabolite in a noninvasive manner.[16,35]

**5.5. Cytotoxicity Testing.** The HEK-293T mammalian cell line was cultured in DMEM supplemented with 10% heat-inactivated FBS and 1% antibiotic−antimycotic cocktail (streptomycin, penicillin, and amphotericin B) in a 5% $CO_2$ humidified chamber at 37 °C. The standard MTT (3-[4,5-dimethylthiazol-2-yl]-2,5-diphenyltetrazolium bromide) assay was applied to estimate the toxicity level of selenium. Concisely, the HEK-293T cells (9000−10,000 cells/well) were plated in a 96-well culture plate. Cultured cells were incubated in a 5% $CO_2$ humidified chamber at 37 °C for 24 h. After 80% of confluency, the media was changed, and the cells were treated with different concentrations of selenium (0−50 $\mu$M) for 12 h. Subsequent to the cultivation time, a mixture of culture medium and selenium was removed from the well, and washing of the wells was done with PBS (pH 7.5). A mixture of serum-free DMEM (100 $\mu$L) and MTT solution (25 $\mu$L) (from 5 mg/mL stock) was cast onto each well and incubated in the $CO_2$ incubator for 4−5 h sat 37 °C. The experiment was recurrent in triplicate. After incubation, the cells were washed and additionally incubated for 4−5 h at 37 °C with incomplete DMEM media (100 $\mu$L) and MTT solution (10 $\mu$L) (taken from 5 mg/mL stock) in the $CO_2$ incubator. The supernatant media of cells were substituted by 150−200 $\mu$L of dimethyl sulfoxide to solubilize the residual black fuzzy crystals (formazan) on the rocker shaker. Formazan was dissolved to provide a purple-blue color. After 30 min, the absorbance of the subsequent solution was measured at 570 nm using a multiplate ELSIA reader (BioRad). The percentage cell viability was valued and designed as a function of the concentration of selenium. In the case of straight imaging, cells were coated in a 12-well cell culture plate and treated with 5 and 10 $\mu$M selenium.

## ■ ASSOCIATED CONTENT

### Supporting Information

The Supporting Information is available free of charge at https://pubs.acs.org/doi/10.1021/acsomega.2c07809.

Dendrograms showing confirmation of mutant variants of SelFS, confocal images showing expression of SelFS in *E. coli*, schematic representations of the SelFS construct designed in the pRSET-B vector, and the Blast sequencing result of SeBP (PDF)

## ■ AUTHOR INFORMATION


### Corresponding Author

**Mohd Mohsin** − *Department of Biosciences, Jamia Millia Islamia, New Delhi 110025, India;* orcid.org/0000-0002-4127-5970; Phone: +91-(11)26981717; Email: mmohsin1@jmi.ac.in; Fax: +91(11)2698 0229

### Authors

**Reshma Bano** − *Department of Biosciences, Jamia Millia Islamia, New Delhi 110025, India*

**Mohammad Zeyaullah** − *Department of Basic Medical Science, College of Applied Medical Sciences, King Khalid University, Abha, Asir 61421, Saudi Arabia*

**Mohammad Suhail Khan** − *Department of Public Health, College of Applied Medical Sciences, King Khalid University, Abha, Asir 61421, Saudi Arabia*

Complete contact information is available at: https://pubs.acs.org/10.1021/acsomega.2c07809


### Author Contributions

R.B., M.M., and M.Z. designed the study and prepared the original manuscript. R.B. and M.M. conducted the experiments and analyzed the *in vitro* and *in vivo* data. R.B., M.M., and M.S.K. analyzed the data and revised the manuscript and approved the final manuscript.

### Notes

The authors declare no competing financial interest.

## ■ ACKNOWLEDGMENTS

The first author (R.B.) kindly acknowledges the University Grants Commission, Govt. of India, for Senior Research Fellowship in the form of MANF (Maulana Azad National Fellowship). The authors extend their appreciation to the Deanship of Scientific Research at King Khalid University,

KSA, for funding this work through a research group program under grant number RGP. 2/181/43.

## REFERENCES

(1) Wilber, C. G. Toxicology of selenium: a review. *Clin. Toxicol.* **1980**, *17*, 171−230.
(2) Zheng, H. Selenium as an essential micronutrient: roles in cell cycle and apoptosis. *Molecules* **2009**, *14*, 1263−1278.
(3) Johnson, C. C.; Fordyce, F. M.; Rayman, M. P. Symposium on 'Geographical and geological influences on nutrition': factors controlling the distribution of selenium in the environment and their impact on health and nutrition. *Proc. Nutr. Soc.* **2010**, *69*, 119−132.
(4) Rosenfeld, I.; Beath, O.A. *Selenium, Geobotany, Biochemistry, Toxicity, and Nutrition*. Academic Press, New York, 1964, 294.
(5) Saito, Y.; Yoshida, Y.; Akazawa, T.; Takahashi, K.; Niki, E. Cell death caused by selenium deficiency and protective effect of antioxidants. *J. Biol. Chem.* **2003**, *278*, 39428−39434.
(6) Zachariadis, A. G.; Kapsimali, D. C.; Rosenberg, E. A Review of Recent Developments in Sample Pretreatment, Separation and Hyphenated Atomic and Mass Spectrometric Techniques for Organo selenium Speciation in Biological Liquids. *Curr. Org. Chem.* **2010**, *14*, 2282−2299.
(7) Cao, G.; Xu, F.; Wang, S.; Xu, K.; Hou, X.; Wu, P. Gold nanoparticle-based colorimetric assay for selenium detection via hydride generation. *Anal. Chem.* **2017**, *89*, 4695−4700.
(8) Ezoe, K.; Ohyama, S.; Hashem, M. A.; Ohira, S. I.; Toda, K. Automated determinations of selenium in thermal power plant wastewater by sequential hydride generation and chemiluminescence detection. *Talanta* **2016**, *148*, 609−616.
(9) Amjadi, M.; Hallaj, T.; Salari, R. A highly sensitive plasmonic sensor for detection of selenium based on the shape transformation of silver nanoprisms. *Sens. Actuators, B* **2018**, *273*, 1307−1312.
(10) Zhaob, X.; Yuana, G.; Dinga, H.; Zhoua, L.; Lina, Q. A TP-FRET-based fluorescent sensor for ratiometric visualization of selenocysteine derivatives in living cells, tissues and zebrafish. *J. Hazard. Mater.* **2020**, *381*, No. 120918.
(11) Cai, D.; Verhey, K. J.; Meyhofer, E. Tracking single kinesin molecules in the cytoplasm of mammalian cells. *Biophys. J.* **2007**, *92*, 4137−4144.
(12) Manley, S.; Gillette, J. M.; Patterson, G. H.; Shroff, H.; Hess, H. F.; Betzig, E.; Lippincott-Schwartz, J. High-density mapping of single-molecule trajectories with photoactivated localization microscopy. *Nat. Methods* **2008**, *5*, 155−157.
(13) Dodani, S. C.; He, Q.; Chang, C. J. A turn-on fluorescent sensor for detecting nickel in living cells. *J. Am. Chem. Soc.* **2009**, *131*, 18020−18021.
(14) Soleja, N.; Mohsin, M. Real time quantification of intracellular nickel using genetically encoded FRET-based nanosensor. *Int. J. Biol. Macromol.* **2019**, *138*, 648−657.
(15) Fehr, M.; Frommer, W. B.; Lalonde, S. Visualization of maltose uptake in living yeast cells by fluorescent nanosensors. *PNAS* **2002**, *99*, 9846−9851.
(16) Mohsin, M.; Ahmad, A. Genetically-encoded nanosensor for quantitative monitoring of methionine in bacterial and yeast cells. *Biosens. Bioelectron.* **2014**, *59*, 358−364.
(17) Malhotra, A. Chapter 16 Tagging for Protein Expression, in: Burgess, RR, Deutscher, MP (Eds), *Guide to Protein Purification*, 2nd Edition, Methods in enzymology. 2009, pp. 239−252.
(18) Miyawaki, A. Development of probes for cellular functions using fluorescent proteins and fluorescence resonance energy transfer. *Annu. Rev. Biochem.* **2011**, *80*, 357−373.
(19) Allan, B. C.; Lacourciere, G. M.; Stadtman, T. C. Responsiveness of selenoproteins to dietary selenium. *Annu. Rev. Nutr.* **1999**, *19*, 1−6.
(20) de Lorimier, R. M.; Smith, J. J.; Dwyer, M. A.; Looger, L. L.; Sali, K. M.; Paavola, C. D.; Rizk, S. S.; Sadigov, S.; Conrad, D. W.; Loew, L.; Hellinga, H. W. Construction of a fluorescent biosensor family. *Protein Sci.* **2002**, *11*, 2655−2675.
(21) Vinkenborg, J. L.; van Duijnhoven, S. M.; Merkx, M. Reengineering of a fluorescent zinc sensor protein yields the first genetically encoded cadmium probe. *Chem. Commun.* **2011**, *47*, 11879−11881.
(22) Suzuki, M.; Lee, D. Y.; Inyamah, N.; Stadtman, T. C.; Tjandra, N. Solution NMR structure of selenium-binding protein from *Methanococcus vannielii*. *J. Biol. Chem.* **2008**, *283*, 25936−25943.
(23) Gruenwald, K.; Holland, J. T.; Stromberg, V.; Ahmad, A.; Watcharakichkorn, D.; Okumoto, S. Visualization of glutamine transporter activities in living cells using genetically encoded glutamine sensors. *PLoS One* **2012**, *7*, No. e38591.
(24) Mohsin, M.; Abdin, M. Z.; Nischal, L.; Kardam, H.; Ahmad, A. Genetically encoded FRET-based nanosensor for in vivo measurement of leucine. *Biosens. Bioelectron.* **2013**, *50*, 72−77.
(25) Soleja, N.; Manzoor, O.; Khan, P.; Mohsin, M. Engineering genetically encoded FRET-based nanosensors for real time display of arsenic ($As^{3+}$) dynamics in living cells. *Sci. Rep.* **2019**, *9*, 11240.
(26) Soleja, N.; Irfan, M. M. Ratiometric imaging of flux dynamics of cobalt with an optical sensor. *J. Photochem. Photobiol., A* **2020**, *400*, No. 112699.
(27) Betolngar, D. B.; Erard, M.; Pasquier, H.; Bousmah, Y.; Diop-Sy, A.; Guiot, E.; Vincent, P.; Merola, F. pH sensitivity of FRET reporters based on cyan and yellow fluorescent proteins. *Anal. Bioanal. Chem.* **2015**, *407*, 4183−4193.
(28) Esposito, A.; Gralle, M.; Dani, M. A.; Lange, D.; Wouters, F. S. Phlameleons: A family of FRET-based protein sensors for quantitative ph imaging. *Biochemistry* **2008**, *47*, 13115−13126.
(29) Van der Krogt, G. N. M.; Ogink, J.; Ponsioen, B.; Jalink, K. A comparison of donor-acceptor pairs for genetically encoded FRET sensors: application to the Epac cAMP sensor as an example. *PLoS One* **2008**, *3*, No. e1916.
(30) Ahmad, M.; Mohsin, M.; Iqrar, S.; Manzoor, O.; Siddiqi, T. O.; Ahmad, A. Live cell imaging of vitamin B12 dynamics by genetically encoded fluorescent nanosensor. *Sens. Actuators, B* **2018**, *257*, 866−874.
(31) Chiu, T. Y.; Chen, P. H.; Chang, C. L.; Yang, D. M. Live-cell dynamic sensing of Cd2+ with a FRET-based indicator. *PLoS One* **2013**, *8*, No. e65853.
(32) Patel, N.; Gold, M. G. The genetically encoded tool set for investigating cAMP: more than the sum of its parts. *Front. Pharmacol.* **2015**, *6*, 164.
(33) Hamilton, S. J. Review of selenium toxicity in the aquatic food chain. *Sci. Total Environ.* **2004**, *326*, 1−31.
(34) Agrawal, N.; Soleja, N.; Bano, R.; Nazir, R.; Siddiqi, T. O.; Mohsin, M. FRET-based genetically encoded sensor to monitor silver ions. *ACS Omega* **2021**, *6*, 4164−14173.
(35) Ahmad, M.; Ameen, S.; Siddiqi, T. O.; Khan, P. Live cell monitoring of glycine betaine by FRET-based genetically encoded nanosensor. *Biosens. Bioelectron.* **2016**, *86*, 169−175.
(36) Olson, O. E.; Palmer, I. S.; Whithead, E. J. Determination of selenium in biological materials, Methods. *Biochem. Anal.* **1973**, *2*, 40.
(37) Jacobs, M.; Frost, C. Toxicological effects of sodium selenite in Sprague-Dawley rats. *J. Toxicol. Environ. Health* **1981**, *8*, 575−585.



https://doi.org/10.1021/acsomega.2c07809
*ACS Omega* 2023, 8, 8625−8633